

On the Inclusion of Charge and Spin States in Cartesian Tensor Neural Network Potentials

Guillem Simeon,[†] Antonio Mirarchi,[†] Raul P. Pelaez,[†] Raimondas Galvelis,^{†,‡} and Gianni De Fabritiis^{*,†,‡,¶}

[†]*Computational Science Laboratory, Universitat Pompeu Fabra, Barcelona Biomedical Research Park (PRBB), C Dr. Aiguader 88, 08003 Barcelona, Spain.*

[‡]*Acellera Labs, C Dr Trueta 183, 08005, Barcelona, Spain*

[¶]*Institució Catalana de Recerca i Estudis Avançats (ICREA), Passeig Lluís Companys 23, 08010 Barcelona, Spain*

E-mail: g.defabritiis@gmail.com

Abstract

In this letter, we present an extension to TensorNet, a state-of-the-art equivariant Cartesian tensor neural network potential, allowing it to handle charged molecules and spin states without architectural changes or increased costs. By incorporating these attributes, we address input degeneracy issues, enhancing the model’s predictive accuracy across diverse chemical systems. This advancement significantly broadens TensorNet’s applicability, maintaining its efficiency and accuracy.

1 Introduction

Neural network potentials,^{1–11} which are deep learning models used to predict the energy and forces of atomic systems,¹² typically rely on atomic numbers and positions as their sole inputs. This simplification, while facilitating model construction and computation, overlooks other significant properties such as total charge and spin state, which are crucial attributes that influence the behavior and interaction of atomistic systems. Furthermore, neglecting total charge and spin state can lead to a degeneracy of inputs.¹³ This degeneracy occurs when different molecular states, distinguishable only by

their charge or spin, are represented by identical inputs for the model, impeding the model’s ability to discern the states and accurately predict potential energies and forces.

In the literature, charges have typically been addressed in neural network potentials with the aim of incorporating long-range electrostatics.^{5,14–17} These approaches provide mechanisms for the global redistribution of charge across the system, utilizing neural networks informed by the chemical environment to predict intermediate properties, such as electronegativities and effective charges, and equilibration schemes¹⁸ that involve solving systems of linear equations,^{13–17} or through self-consistent processes.¹⁹ Furthermore, in some cases, additionally predicted quantities such as atomic charges are used for the computation of manually introduced physics-based terms in the energy prediction.^{5,13}

In this work, we introduce a simple yet effective extension to TensorNet,²⁰ a state-of-the-art equivariant neural network potential based on Cartesian tensors, enabling it to accommodate charged molecules and spin states. This modification does not require any architectural changes to the original model, nor does it lead to increased computational costs. Even though the approach does not explicitly account for global redistribution of properties, this en-

hancement retains the model’s original predictive accuracy on the systems we studied, and the approach circumvents the need for explicit physical terms or the prediction of additional quantities. This enhancement expands TensorNet’s applicability to a broader range of chemical systems.

2 Method

Given some input atomic numbers and positions $\{Z, \mathbf{r}\}$, TensorNet learns for every atom (i) a set of rank-2 tensors (3x3 matrices) $X^{(i)}$. TensorNet’s operations make these representations equivariant to rotations and reflections of the input, meaning that given some matrix $R \in O(3)$, when the matrix is applied on input positions $\{\mathbf{r}\} \rightarrow R\{\mathbf{r}\}$, atomic representations transform as $X^{(i)} \rightarrow RX^{(i)}R^T$, where R^T denotes the transpose of R . Furthermore, $X^{(i)}$ can be decomposed into scalar, vector, and symmetric traceless components, $I^{(i)}$, $A^{(i)}$ and $S^{(i)}$, respectively. After several message-passing layers, the squared Frobenius norms of the representations, which are invariant under $O(3)$, are further processed by the neural network to predict energies, obtaining atomic forces via automatic differentiation.

One of the key operations in TensorNet is how neighboring nodes’ tensor features are aggregated and used together with the ones of the receiving node to generate a new set of node tensor representations that transform appropriately under $O(3)$. We refer the reader to Ref 20 for full details. In each layer, after some node level transformations $X^{(i)} \rightarrow X'^{(i)} = X^{(i)} / (\|X^{(i)}\| + 1) \rightarrow Y^{(i)}$, pair-wise messages $M^{(ij)}$ from neighbor (j) to receiving atom (i) are built by decomposing neighbor’s features $Y^{(j)}$,

$$M^{(ij)} = \phi(r_{ij})(f_I^{ij}I^{(j)} + f_A^{ij}A^{(j)} + f_S^{ij}S^{(j)}) \quad (1)$$

where f_I^{ij} , f_A^{ij} , f_S^{ij} are learnable functions of the distance between atoms r_{ij} , and $\phi(r_{ij})$ is a cosine cutoff function. Messages are summed for all neighbors, $M^{(i)} = \sum_j M^{(ij)}$, and the generation of new features $Y'^{(i)}$ from current node

features $Y^{(i)}$ and message $M^{(i)}$ is performed via simple matrix product as

$$Y'^{(i)} = Y^{(i)}M^{(i)} + M^{(i)}Y^{(i)}, \quad (2)$$

effectively mixing scalars, vectors, and tensors, and ensuring $O(3)$ -equivariance, as proved in Ref 20. Resulting representations are eventually manipulated to yield residual updates $\Delta X'^{(i)}$ to the layer’s input normalized features $X'^{(i)}$

$$X^{(i)} \leftarrow X'^{(i)} + \Delta X'^{(i)} + (\Delta X'^{(i)})^2, \quad (3)$$

using $X^{(i)}$ to feed the following layer and restart the process.

We propose to include molecular states’ information $\{\psi_k\}$, labeled by k , by modifying Equations (2) and (3) in TensorNet’s interaction layers in the following node-wise manner

$$Y'^{(i)} = (1 + \sum_k \lambda_k \psi_k)(Y^{(i)}M^{(i)} + M^{(i)}Y^{(i)}), \quad (4)$$

$$X^{(i)} \leftarrow X'^{(i)} + \Delta X'^{(i)} + (1 + \sum_k \tilde{\lambda}_k \psi_k)(\Delta X'^{(i)})^2 \quad (5)$$

where λ_k , $\tilde{\lambda}_k$ can be regarded as per-layer constant or learnable weights for the encoding of states such as total charge or spin $\psi_k = \{Q, S, \dots\}$. Notice that the modification does not break equivariance under $O(3)$, since it amounts to a rescaling of tensor features by means of a state-dependent scalar factor. Furthermore, it has been designed in such a way that when the system is neutral and in its singlet state, i.e.

$$Q = S = 0, \quad (6)$$

the model defaults to the original TensorNet (Eqs (2) and (3)), therefore recovering the predictive accuracy already demonstrated in Ref 20.

It is also worth mentioning that, since the inclusion of states is performed node-wise, one can also incorporate atomic attributes, such as partial charges $q^{(i)}$. In this case, one needs to rely on some external partial charge computation scheme, which might assume the avail-

ability of information beyond atomic numbers and positions, such as SMILES representations, molecular bonds’ topology or other preprocessing steps.

3 Results and discussion

We performed a series of experiments with the extended TensorNet model using the TorchMD-Net framework.²¹ We trained the model on a custom-made dataset and on two publicly available datasets, targeting atomic number and geometry degeneracy, as well as the simultaneous presence of neutral and charged molecules regardless of structural or geometric overlap between these. We used a generic set of reasonable hyperparameters, without addressing dataset-dependent fine-tuning to obtain the best possible performances. In all cases, we used the direct model prediction of energies and forces (when needed), without the manual inclusion of physics-based terms. Overall, we evaluate TensorNet’s extension when dealing with total charges, Gasteiger partial charges, or singlet and triplet states.

3.1 Toy degeneracy problem

As a first test, to illustrate the input degeneracy issue and how TensorNet’s extension resolves it without affecting its baseline accuracy, we constructed two toy datasets, Dataset A and Dataset B, each one comprising five members of five pairs of unique molecular systems, each of the elements in the pair differing in total charge (see Fig 1). These pairs are indistinguishable to a neural network that does not account for total charge, as they share identical atomic numbers and geometric configurations. The datasets include total charges, Gasteiger partial charges computed with RDKit, and calculated energies and atomic forces for 2000 conformers per molecule using GFN2-xTB.²² Therefore, each dataset contains a total of 10k data points. Conformers were generated by minimizing each molecule, displacing atomic positions with Gaussian noise with a standard deviation of 0.2 Å, and filtering them such that

maximum atomic forces are <100 eV/Å.

The logic behind the experiment is the following: when training the original TensorNet on each dataset separately, the learning should proceed as expected, with the network successfully learning the mapping between the atomic inputs and the output properties. However, when the datasets are combined, the inability to distinguish charge states leads to an overlap in the input space, being mapped to different values of energies and forces. As a result, the network should fail to learn accurately. On the other hand, the extension of the model should allow the network to learn accurately the mapping between inputs and outputs in all cases.

Splits of 50/10/40% were used for training, validation, and testing, respectively, both for single and combined datasets. For the charge-aware case, we tried separately the inclusion of total charges Q and Gasteiger partial charges $q^{(i)}$, both with $\lambda_Q = \tilde{\lambda}_Q$ and $\lambda_{q^{(i)}} = \tilde{\lambda}_{q^{(i)}}$ equal to 0.1 across all layers. Results can be found in Table 1. As expected, the original model trained on the merged dataset has a very poor accuracy (TensorNet, Dataset $A \cup B$). The extension with total and partial charges allows us to learn the merged dataset with sub-meV and sub-meV/Å differences in energy and force errors with respect to single dataset training of the corresponding extended model. Moreover, the use of total charge Q gives better results than the use of partial charges $q^{(i)}$, since errors on the merged dataset and dataset A are lower.

3.2 SPICE PubChem

The PubChem subset inside the SPICE dataset²³ (version 1.1.4) consists of conformers of small drug-like molecules, with energies and forces computed at the ω B97M-D3(BJ)/def2-TZVPPD level of theory. Approximately 4% of the molecules and conformers in the dataset are not neutral. The dataset already provides total charges, while we computed Gasteiger partial charges for all the molecules in the subset, including the neutral ones. The computation of partial charges failed with RDKit for 42 molecules, with corresponding conformers being discarded. This resulted in 707,558 data

Table 1: **Toy datasets results.** Energy (E) and forces (F) mean absolute errors in meV and meV/Å.

Model		Dataset A	Dataset B	Dataset A \cup B
TensorNet	E (meV)	2.6	2.3	4437
	F (meV/Å)	11.6	14.3	772
TensorNet+0.1 Q	E (meV)	2.4	2.3	2.5
	F (meV/Å)	11.9	14.8	13.9
TensorNet+0.1 $q^{(i)}$	E (meV)	2.8	2.3	3.2
	F (meV/Å)	13.7	14.9	14.8

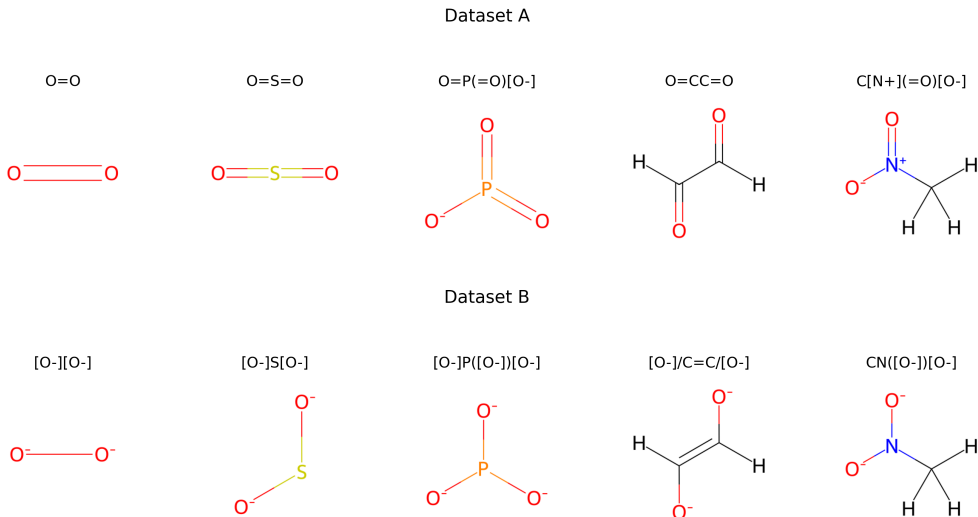


Figure 1: Molecules included in the A and B toy datasets, from which 2,000 data points per molecule are obtained by generating conformers and computing potential energies and atomic forces using GFN2-xTB.²² Columns illustrate degenerate pairs of molecules for a neural network that uses solely atomic numbers and positions as inputs.

points in total.

To include total charge Q or atomic partial charges $q^{(i)}$, we take $\lambda_Q = \tilde{\lambda}_Q$ and $\lambda_{q^{(i)}} = \tilde{\lambda}_{q^{(i)}}$ constant and non-learnable across all layers, equal to 0.1 or 0.25. We used 80/10/10% splits for training, validation, and testing, respectively. In Table 2, we show that including total charge Q or partial charges $q^{(i)}$ can improve energy and forces accuracy. Even though charged species comprise only 4% of the data points, the freedom given to the model to adapt to varying charge states improves significantly the accuracy on both charged and neutral conformations. With the best method, which uses total charge Q with $\lambda_Q = \tilde{\lambda}_Q = 0.1$, reductions of 30% and 12% in energy errors are achieved for charged and neutral test molecules, respectively. Nevertheless, the inclusion of Gasteiger

partial charges gives relevant out-of-the-box improvements too.

3.3 QMspin

The QMspin dataset, introduced in Ref 24, includes molecules optimized in both singlet and triplet states. The dataset, drawn from the QM9 database, provides a comprehensive collection of around 13,000 carbene structures, with energies calculated for both singlet and triplet states. Therefore, QMspin contains approximately 26,000 data points. The singlet and triplet energy information enables the assessment of the model’s predictive performance on spin state differences, an aspect previously unaddressed due to the degeneracy of inputs, allowing us to test and validate TensorNet’s ex-

Table 2: **SPICE PubChem results.** Energy (E) and forces (F) mean absolute errors in meV and meV/Å, on the entire test set, and separately on neutral and charged conformations in the test set. Q refers to total charge while $q^{(i)}$ refers to Gasteiger partial charges, with factors corresponding to weights $\lambda_Q = \tilde{\lambda}_Q$ and $\lambda_{q^{(i)}} = \tilde{\lambda}_{q^{(i)}}$, respectively.

Model		Test total	Test neutral	Test charged
TensorNet	E (meV)	34.2	32.7	70.1
	F (meV/Å)	34.7	33.8	58.4
TensorNet+0.1 $q^{(i)}$	E (meV)	31.5	30.5	55.2
	F (meV/Å)	33.9	33.0	56.7
TensorNet+0.25 $q^{(i)}$	E (meV)	30.5	29.6	50.4
	F (meV/Å)	32.9	32.1	55.6
TensorNet+0.1 Q	E (meV)	29.4	28.6	49.3
	F (meV/Å)	31.4	30.6	50.1
TensorNet+0.25 Q	E (meV)	29.6	28.6	52.0
	F (meV/Å)	31.6	30.6	52.9

tension beyond charged states. We incorporate singlet or triplet states as $S = 0$ and $S = 1$, respectively, and $\lambda_S = \tilde{\lambda}_S = 0.1$ for all layers.

We removed 228 data points, which corresponded to geometry files where the number of atoms in the header did not match the number of atoms with coordinate entries. Following Ref 13, we used 20,000 and 1,000 data points for training and validation, respectively, being the remaining ones used for testing. Results, found in Table 3, show that the inclusion of the spin state S , and therefore degeneracy breaking, improves 10-fold the accuracy of the model, achieving 43 meV error in energies, which is approximately equivalent to 1 kcal/mol, considered chemical accuracy. Furthermore, this represents an improvement of $\sim 40\%$ with respect to SpookyNet,¹³ the only model that to the best of our knowledge has been benchmarked with the QMspin dataset.

Table 3: **QMspin results.** Comparison of mean absolute errors on the QMspin test set, in meV. S refers to spin state, with the factor corresponding to $\lambda_S = \tilde{\lambda}_S = 0.1$.

SpookyNet	TensorNet	TensorNet+0.1 S
68 meV	432 meV	43 meV

4 Conclusion

In this letter, we have introduced a simple extension to TensorNet allowing it to handle charge and spin states. These attributes have typically been disregarded in state-of-the-art neural network potentials, which operate solely with atomic numbers and positions, leading to degeneracies in input space. Specifically, through a series of experiments, we have demonstrated the model’s improved accuracy and its broader applicability to a range of chemical systems.

This work opens the path to potential improvements. These results assume that additional attributes are scaled by a constant number. It would be worth exploring different strategies, such as making them learnable single or channel-wise scalars, potentially depending on other atomic properties such as atomic numbers. Another important aspect is that, when using partial charges, conformation-agnostic schemes have a dependence on molecular topology, which needs to be guessed from atomic coordinates, as opposed to total charge.

However, in light of the results we have so far obtained, we conclude that the approach presented in this letter represents a significant zero-cost enhancement for TensorNet, as well as an important message to take into account for future architectures.

Data and software availability

TensorNet and its extension can be found within TorchMD-Net: <https://github.com/torchmd/torchmd-net>. The toy datasets have been made available at <https://zenodo.org/records/10852523>. The SPICE dataset version 1.1.4 is publicly available at <https://zenodo.org/records/8222043>. The QM-spin dataset is available at <https://archive.materialscloud.org/record/2020.0051/v1>.

Acknowledgments

G. S. is financially supported by Generalitat de Catalunya’s Agency for Management of University and Research Grants (AGAUR) PhD grant FI-2-00587. Research reported in this publication was supported by the project PID2020-116564GB-I00, has been funded by MICIU/AEI /10.13039/501100011033, and by the National Institute of General Medical Sciences (NIGMS) of the National Institutes of Health under award number R01GM140090. The content is solely the responsibility of the authors and does not necessarily represent the official views of the National Institutes of Health.

References

- (1) Behler, J.; Parrinello, M. Generalized Neural-Network Representation of High-Dimensional Potential-Energy Surfaces. *Phys. Rev. Lett.* **2007**, *98*, 146401.
- (2) Kocer, E.; Ko, T. W.; Behler, J. Neural Network Potentials: A Concise Overview of Methods. 2021.
- (3) Smith, J. S.; Isayev, O.; Roitberg, A. E. ANI-1: an extensible neural network potential with DFT accuracy at force field computational cost. *Chemical Science* **2017**, *8*, 3192–3203.
- (4) Schütt, K. T.; Sauceda, H. E.; Kindermans, P.-J.; Tkatchenko, A.; Müller, K.-R. SchNet – A deep learning architecture for molecules and materials. *The Journal of Chemical Physics* **2018**, *148*.
- (5) Unke, O. T.; Meuwly, M. PhysNet: A Neural Network for Predicting Energies, Forces, Dipole Moments, and Partial Charges. *Journal of Chemical Theory and Computation* **2019**, *15*, 3678–3693.
- (6) Deringer, V. L.; Caro, M. A.; Csányi, G. Machine Learning Interatomic Potentials as Emerging Tools for Materials Science. *Advanced Materials* **2019**, *31*, 1902765.
- (7) Schütt, K. T.; Unke, O. T.; Gastegger, M. Equivariant message passing for the prediction of tensorial properties and molecular spectra. 2021; <https://arxiv.org/abs/2102.03150>.
- (8) Thölke, P.; Fabritiis, G. D. Equivariant Transformers for Neural Network based Molecular Potentials. International Conference on Learning Representations. 2022.
- (9) Batzner, S.; Musaelian, A.; Sun, L.; Geiger, M.; Mailoa, J. P.; Kornbluth, M.; Molinari, N.; Smidt, T. E.; Kozinsky, B. E(3)-equivariant graph neural networks for data-efficient and accurate interatomic potentials. *Nature Communications* **2022**, *13*.
- (10) Musaelian, A.; Batzner, S.; Johansson, A.; Sun, L.; Owen, C. J.; Kornbluth, M.; Kozinsky, B. Learning local equivariant representations for large-scale atomistic dynamics. *Nature Communications* **2023**, *14*.
- (11) Batatia, I.; Kovacs, D. P.; Simm, G. N. C.; Ortner, C.; Csanyi, G. MACE: Higher Order Equivariant Message Passing Neural Networks for Fast and Accurate Force Fields. Advances in Neural Information Processing Systems. 2022.
- (12) Duval, A.; Mathis, S. V.; Joshi, C. K.; Schmidt, V.; Miret, S.; Malliaros, F. D.;

- Cohen, T.; Liò, P.; Bengio, Y.; Bronstein, M. A Hitchhiker’s Guide to Geometric GNNs for 3D Atomic Systems. 2023; <https://arxiv.org/abs/2312.07511>.
- (13) Unke, O. T.; Chmiela, S.; Gastegger, M.; Schütt, K. T.; Saucedo, H. E.; Müller, K.-R. SpookyNet: Learning force fields with electronic degrees of freedom and nonlocal effects. *Nature Communications* **2021**, *12*.
- (14) Ghasemi, S. A.; Hofstetter, A.; Saha, S.; Goedecker, S. Interatomic potentials for ionic systems with density functional accuracy based on charge densities obtained by a neural network. *Phys. Rev. B* **2015**, *92*, 045131.
- (15) Faraji, S.; Ghasemi, S. A.; Rostami, S.; Rasoulkhani, R.; Schaefer, B.; Goedecker, S.; Amsler, M. High accuracy and transferability of a neural network potential through charge equilibration for calcium fluoride. *Phys. Rev. B* **2017**, *95*, 104105.
- (16) Ko, T. W.; Finkler, J. A.; Goedecker, S.; Behler, J. A fourth-generation high-dimensional neural network potential with accurate electrostatics including non-local charge transfer. *Nature Communications* **2021**, *12*.
- (17) Shaidu, Y.; Pellegrini, F.; Küçükbenli, E.; Lot, R.; de Gironcoli, S. Incorporating long-range electrostatics in neural network potentials via variational charge equilibration from shortsighted ingredients. *npj Computational Materials* **2024**, *10*.
- (18) Rappe, A. K.; Goddard, W. A. Charge equilibration for molecular dynamics simulations. *The Journal of Physical Chemistry* **1991**, *95*, 3358–3363.
- (19) Gao, A.; Remsing, R. C. Self-consistent determination of long-range electrostatics in neural network potentials. *Nature Communications* **2022**, *13*.
- (20) Simeon, G.; De Fabritiis, G. TensorNet: Cartesian Tensor Representations for Efficient Learning of Molecular Potentials. *Advances in Neural Information Processing Systems*. 2023; pp 37334–37353.
- (21) Pelaez, R. P.; Simeon, G.; Galvelis, R.; Mirarchi, A.; Eastman, P.; Doerr, S.; Thölke, P.; Markland, T. E.; De Fabritiis, G. TorchMD-Net 2.0: Fast Neural Network Potentials for Molecular Simulations. 2024; <https://arxiv.org/abs/2402.17660>.
- (22) Bannwarth, C.; Ehlert, S.; Grimme, S. GFN2-xTB—An Accurate and Broadly Parametrized Self-Consistent Tight-Binding Quantum Chemical Method with Multipole Electrostatics and Density-Dependent Dispersion Contributions. *Journal of Chemical Theory and Computation* **2019**, *15*, 1652–1671.
- (23) Eastman, P.; Behara, P. K.; Dotson, D. L.; Galvelis, R.; Herr, J. E.; Horton, J. T.; Mao, Y.; Chodera, J. D.; Pritchard, B. P.; Wang, Y.; De Fabritiis, G.; Markland, T. E. SPICE, A Dataset of Drug-like Molecules and Peptides for Training Machine Learning Potentials. *Scientific Data* **2023**, *10*.
- (24) Schwilk, M.; Tahchieva, D. N.; von Lilienfeld, O. A. Large yet bounded: Spin gap ranges in carbenes. 2020; <https://arxiv.org/abs/2004.10600>.

A Hyperparameters

All experiments were performed on two NVIDIA RTX 4090 using PyTorch Lightning’s DDP multi-GPU training protocol.

Table 4: Toy datasets hyperparameters.

Parameter	Value
activation	silu
batch_size	16
cutoff_lower	0.0
cutoff_upper	5.0
derivative	True
early_stopping_patience	100
embedding_dimension	128
equivariance_invariance_group	0(3)
gradient_clipping	40
lr	1e-3
lr_factor	0.5
lr_min	1e-7
lr_patience	15
lr_warmup_steps	0
neg_dy_weight	10.0
num_layers	2
num_rbf	32
seed	1
train_size	0.5
val_size	0.1
y_weight	1.0

Table 5: SPICE PubChem hyperparameters.

Parameter	Value
activation	silu
batch_size	64
cutoff_lower	0.0
cutoff_upper	5.0
derivative	True
early_stopping_patience	50
embedding_dimension	128
equivariance_invariance_group	0(3)
gradient_clipping	100
lr	1e-3
lr_factor	0.5
lr_min	1e-7
lr_patience	5
lr_warmup_steps	0
neg_dy_weight	10.0
num_layers	2
num_rbf	32
seed	1
train_size	0.8
val_size	0.1
y_weight	1.0

Table 6: QMspin hyperparameters.

Parameter	Value
activation	silu
batch_size	16
cutoff_lower	0.0
cutoff_upper	5.0
derivative	False
early_stopping_patience	100
embedding_dimension	128
equivariance_invariance_group	0(3)
gradient_clipping	40
lr	1e-3
lr_factor	0.5
lr_min	1e-7
lr_patience	30
lr_warmup_steps	0
neg_dy_weight	0.0
num_layers	2
num_rbf	32
seed	1
train_size	20000
val_size	1000
y_weight	1.0